Heliyon 10 (2024) e38638

Contents lists available at ScienceDirect

Heliyon

journal homepage: www.cell.com/heliyon

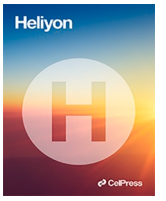

Research article

Experimental and modeling approaches to determine drug diffusion coefficients in artificial mucus

Ashley C. Wynne [a], Brandon S. Abbott [b], Reza Niazi [c], Kayla Foley [d], Keisha B. Walters [d,*]

[a] Sealed Air Corporation, 2405 Cascade Pointe Blvd, Charlotte, NC, 28208, USA
[b] School of Chemical, Biological and Materials Engineering, The University of Oklahoma, Norman, OK, 73019, USA
[c] Department of Mathematics, The University of Oklahoma, Norman, OK, 73019, USA
[d] Ralph E. Martin Department of Chemical Engineering, University of Arkansas, Fayetteville, AR, 72701, USA

ARTICLE INFO

Keywords:
Albuterol
Theophylline
Diffusion coefficient
Fourier transform infrared spectroscopy
Artificial mucus

ABSTRACT

Asthma, usually characterized by inflammation and mucus accumulation, causes restricted airflow and impaired lung function. The physiological and biochemical characteristics of mucus pose a strong barrier for drugs administered orally or via the pulmonary route for asthma treatment. In this study, two drugs commonly employed in the treatment of asthma, theophylline and albuterol, were placed in contact with an artificial mucus layer, measuring their interface concentrations, and modeling the concentration profiles to determine their diffusion coefficients. To monitor the diffusion process, the upper surface of a mucus layer was placed in contact with the drug solutions and the lower mucus surface was in contact with a zinc selenide crystal to allow for time-resolved Fourier transform infrared spectroscopy (FTIR) measurements. FTIR spectra were collected at constant time intervals and monitored for quantitative changes in spectral peaks corresponding to functional groups specific to each of these drugs. Changes in peak heights were correlated to concentration via Beer's Law. Fick's 2nd Law of Diffusion was used along with Crank's trigonometric series solution for a planar semi-infinite sheet to analyze the concentration data and determine diffusion coefficients. Using this method, fitting the experimental data resulted in diffusivity coefficients of $D = 6.56 \times 10^{-6}$ cm^2/s for theophylline and $D = 4.66 \times 10^{-6}$ cm^2/s for albuterol through artificial mucus. The drug diffusivity coefficients align closely with literature reports, wherein, diffusivity data was obtained experimentally using a rotating-disk apparatus and intrinsic dissolution technique. By coupling analytical and experimentally determined drug diffusion data, this approach provides a fast, non-invasive method for quickly assessing drug diffusion profiles through complex media.

1. Introduction

Asthma, a chronic inflammatory condition of the lung airways resulting in constriction of the surrounding muscles and obstruction of airflow to and from the lung, is a leading respiratory illness that carries an economic burden in the US alone of over $81 billion annually [1,2] with over 358.2 million individuals affected by asthma globally [3]. Current therapeutic options for asthma consist

* Corresponding author.
E-mail address: keisha.walters@uark.edu (K.B. Walters).

https://doi.org/10.1016/j.heliyon.2024.e38638
Received 15 March 2024; Received in revised form 10 September 2024; Accepted 26 September 2024
Available online 27 September 2024

primarily of aerosolized inhalation pharmaceuticals that range from fast-acting rescue drugs to long-term medications that prevent lung inflammation and provide disease control [4]. The implementation of inhalation aerosol drugs has been one of the most successful and effective treatments for combatting respiratory illnesses. In weighing alternative therapeutic pathways, pulmonary drug delivery routes (e.g., inhalation therapies) possess several characteristics that make them suited for further investigation and development, namely improved patient compliance, rapid onset of action, hepatic and intestinal avoidance, minimal invasiveness/needle-free systemic drug administration, better chemical stability, and smaller required drug dosages [5–11]. Studies suggest that due to the slow clearance and immense surface area of the pulmonary system, the lungs provide a significant increase in bioavailability for macromolecules when compared to all other entry ports of the body [10]. Although significant progress has been made in evaluating both structural and functional lung features involved in drug uptake, absorption mechanisms remain poorly understood and difficult to quantify.

Improved therapeutic options and advanced drug delivery systems for respiratory diseases necessitates better understanding of the particulates' path—including inhalation drugs—through the respiratory tract, deposition patterns, and bioavailability. A more comprehensive understanding of the pulmonary system can directly enhance drug delivery/design, enabling time-release strategies and site-specific application, which results in cheaper associated costs, decreased drug dosage, and minimized invasiveness to the body. In the case of inhalation therapies, drug particles travel through the bronchiole lung generations and ultimately contact the mucus layer that coats the alveolar pulmonary membrane. Inhaled drugs must then diffuse through the mucus layer to reach the lung surface and treat the inflammation. The complexity of the mucus is a major contributing factor to the path of the drug particulates and the composition of the pulmonary mucus layer. Mucus is hydrophobic in nature [12], consists of two layers, and is arranged in crosslinked and entangled mucin fiber networks that effectively protect the lung surface and trap foreign matter entering the lungs. As a result of these innate complexities associated with pulmonary drug delivery, identifying and evaluating experimental and analytical techniques to elucidate diffusivity through complex media, deposition patterns, and physiological drug interactions are critical to optimizing drug design and delivery strategies.

Aerosol drugs are designed to retain medicinal properties while diffusing through the mucus. Drug properties, such as material size, greatly influence the rate of diffusion. Nanoparticles (with effective diameter >100 nm) can remain in the lungs for weeks due to their small size, while larger particles of ideal aerodynamic diameter for treating airways, ca. 1–5 μm [13], are cleared from the lung within 24 h [14]. Particles small enough to diffuse are cleared through the mucus layer, eventually becoming systemic. Larger particles are swept away by cilia or exhaled. It is possible to design particles to overcome the obstruction of the mucus layer. Mucus-inert polymers or hydrophilic coatings can be used to increase the rate of particle diffusion as well as further customize the drug release and improve drug effectiveness [15]. Another technique being investigated is mucoadhesion, where particles are coated with a polymeric material designed to cling to the mucus layer, slowing the particle transfer time and improving drug absorption [15]. By using representative drug-doped solutions and an artificial mucus layer, materials and transport parameters can be examined as part of efforts to model the behavior of drug particles in the human lung.

In addition to size, drug diffusion is also affected by other drug characteristics such as surface charge [12,16], molecular weight, lipophilicity [16], and hydrophilicity [12,17]. Particle charge has been found to influence drug diffusion since mucus components are negatively charged. Khanvilkar et al. reported that positively charged low molecular weight drugs bind to the mucus electrostatically [12]. Modulations in pH contribute to such surface charge effects with increasing pH producing an increase in diffusion coefficient and a decrease in lag time [18]. Alternatively, negatively charged particles are reported to not be affected by the mucus barrier [12,17]. Molecular weight has also been investigated for its influence on particle diffusion. Larhed et al. found that drugs with higher molecular weight had lower diffusion coefficients [16], and this inverse relationship between molecular weight and diffusion coefficient has been reported [12]. Lipophilic and hydrophilic properties of drugs strongly impact their diffusivity as well. Strongly lipophilic particles exhibit lower diffusion coefficients [16], and hydrophobic particles have exhibited lower permeabilities due to mucus's hydrophobic nature [12,17].

Along with research on current and developing treatments for asthma, other factors affecting the efficiency of aerosol treatments need to be investigated to result in the most effective treatment for lung inflammation. Saliva, which acts as a carrier of aerosols to the lungs, needs to be considered when engineering aerosol drugs, as well as the pulmonary mucus that serves as a protective barrier for the lungs while obstructing the diffusion of the drugs to the lung surface. Drugs need to be designed to diffuse through the viscous mucus layer quickly while retaining their medicinal properties. Model mucus membranes have been developed, as well as mathematic simulation models for the diffusion of drugs through mucus. Theophylline was one of the most widely used treatments for asthma for

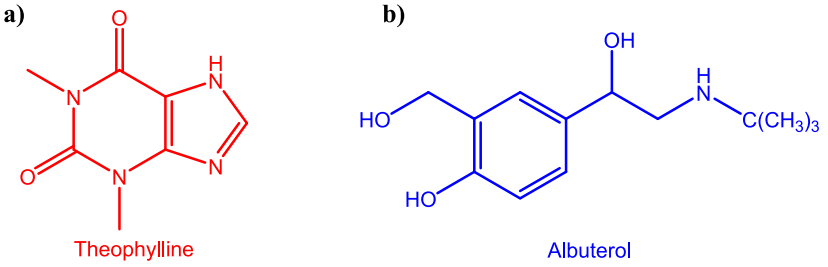

Fig. 1. Chemical structures of a) theophylline and b) albuterol.

decades as both a fast-acting and long-acting treatment; however, due to misuse, abuse, toxicity with high doses, and difficulty determining the optimal dosage other drug solutions are being explored [4].

Theophylline is still used as a long-term treatment but with increased patient monitoring. Albuterol, also known as salbutamol, is mostly used in rescue situations as a response to an asthma attack. Albuterol is one of the most effective immediate treatments when inhaled via aerosol inhaler since it provides a direct effect on the inflamed bronchial smooth muscle. Potassium iodide (KI), an expectorant, is another treatment that thins mucus secretions in the respiratory tract, making it easier for patients to clear the airway by coughing; however, KI is not a commonly used treatment for asthma. This research focuses on determining the effective diffusivity of two asthma treatments: albuterol/salbutamol and theophylline. The chemical structures of these drugs can be seen in Fig. 1 for theophylline (Fig. 1a) and albuterol (Fig. 1b).

1.1. Mucus diffusion using attenuated total reflectance Fourier transform infrared spectroscopy

Conventional methods for analyzing diffusion in transport experiments include dynamic gravimetric sorption and permeation cells [19,20]. Attenuated total reflectance Fourier transform infrared spectroscopy (ATR-FTIR) is a technique that has been used as a method for measuring diffusion [21]. ATR-FTIR allows for noninvasive time-resolved analysis of chemically unique molecular signatures while the diffusion process occurs, as well as quantification of molecular interactions between the diffusing species and the matrix/medium through shifts in IR spectra [19,20,22]. Several systems have successfully utilized time-resolved ATR-FTIR spectra for measuring diffusion. Hallinan et al. measured the diffusion of methanol and water in Nafion using the ATR-FTIR method, as well as relating the spectral information to concentration and, subsequently, Fick's second law. Results of the methanol and water diffusion in Nafion matched results determined from a permeation cell, validating this technique for that material system [19,20]. More recently, Hallinan et al. expanded this work to examine the diffusion of lithium-ion salts in solid polyelectrolytes [23]. Additionally, systems such as water in polymers like poly(vinyl chloride) or poly(ethylene terephthalate) [21], urea through viscose biopolymer films [24], and even biological systems such as the permeation of acetonitrile and *p*-cyanophenol in polyethylene glycol through silastic membranes representative of skin [25] or NSAID drug molecules through acrylic-based transdermal patches [26] have been successfully evaluated using the ATR-FTIR method of data collection and the Fickian diffusion model. Elabd et al. highlight more than fifty systems, primarily diffusants/solutes through polymers, for which this technique has worked [21].

Although FTIR spectroscopy has been used in characterizing diffusion coefficients in polymer systems [20,21,27–29], there are limited examples of this technique being used for analyzing diffusion in mucosal systems. Several extensive reviews detailing common methods used to interrogate mucosal permeability with emphasis on drug diffusion through various mucus systems are provided by Khanvilkar et al. [12], Cu et al. [30], and Newby et al. [31]. In general, the most common methods for measuring small molecule diffusion through mucosal membranes primarily involve measuring the transport through a mucus plug between a source and sink reservoir chamber or tracking of fluorescent or radioactively tagged solute molecules through a finite mucus volume [12,30]. While the experimental setup for the reservoir chamber diffusion measurements is relatively simple, the experiments generally involve long measurement times which can lead to mucus gel structural alterations or partial dissolution, impacting the measured average diffusion coefficients. Diffusion measurements of labeled drug molecules, biomaterials, and nanoparticles through smaller mucus volumes can reduce the impact of mucus alteration on the measured diffusion coefficients and lead to smaller experimental times [30]. Several studies have utilized this latter method for mucosal diffusion using fluorescent microscopy, radioactive measurements, or spectroscopy. For instance, Larhed et al. determined the diffusion coefficients of lipophilic drugs mannitol, metoprolol, propranolol, hydrocortisone, and testosterone through native pig intestinal mucus using a radiolabeled drug tracer and subsequent radioactivity measurements of the sub-sectioned mucus membrane [16]. Fluorescently labeled probes or tagged particles have been used with fluorescent imaging and particle tracking to measure diffusion through human mucus [32,33]. However, these methods require invasive chemical modification of either the diffusant or the mucus layer to fluorescently or radioactively track the solute transport. The chemical modification can also impact the resulting diffusion coefficients [30].

Spectroscopic techniques offer the potential for non-invasive evaluation of solute diffusion in mucosal systems using the unique chemical signatures of the drug molecules without chemical modification. A UV spectrophotometric technique was reported by Owen et al. [34] where two quartz capillary cells, one loaded with nonoxynol-9-doped alginate delivery gel and the other with bovine cervical mucus, were brought into contact with one another to generate quantifiable concentration profiles. Similar UV–vis spectroscopy studies may be applied for UV-active or visible light-absorbing molecules. More recently, pulsed gradient spin-eco NMR has been reviewed as a non-invasive method to evaluate diffusion coefficients in mucosal systems, but requires strong paramagnetic or spin-active nucleus signals [30,35]. ATR-FTIR offers the potential as a non-invasive method to track drug diffusion using the drug's own infrared chemical signatures through a more generally available benchtop method.

While there have been advances made in the synthesis of new inhalation drugs and drug delivery systems, there has been limited research conducted on inhalation-based development of drug diffusion through the mucus layer covering the lung epithelium. The work presented here involves developing methods for measuring diffusion coefficients in artificial mucus, which is important in the modeling and application of drug transport within the lung airways, deposition, and ultimate fate within the lung. Moreover, the work utilizes a commonly used non-invasive spectral characterization technique (ATR-FTIR) combined with nonlinear regression analysis of Fickian diffusion performed in widely available Microsoft Excel software, making the solution a readily assessable solution for other mucosal drug diffusion studies. The specific objectives of this effort are to (1) develop a method to quantify drug concentration in mucus using FTIR and (2) measure the diffusion coefficients of solvent and drug-doped solutions through artificial mucus layers. An artificial mucus, representative of human pulmonary mucus, was used as a surrogate for the native mucus layer present on the lung surface. The composition, structural properties, and rheology of the artificial mucus are not investigated in this work, as these aspects

have been studied in previous research [36]. To achieve the goals of this work, two commonly used drugs in asthma treatments, albuterol and theophylline, were dissolved in isopropanol. These drug-doped IPA solutions were used as a model for a drug-solvent mixture that would be deposited on the mucus surface after inhalation treatments (e.g., nebulized drug solutions) were administered. Overall, this study emphasizes a comprehensive approach that combines rapid, non-invasive analytical methods with experimental techniques to evaluate drug diffusion data, aiming to mitigate the challenges encountered in early drug discovery.

2. Experimental procedures

2.1. Diffusants

Theophylline (>98 %, TCI America, CAS 58-55-9, M.W. 180.17 g/mol) and albuterol (Spectrum, CAS 18559-94-9, M.W. 239.31 g/mol) solutions were prepared at various concentrations using isopropanol (IPA, 70 % v/v aqueous solution, Ricca Chemical, CAS 67-63- 0). Each solution was sonicated using a Branson 3510 sonicator with heat until completely dissolved. Solutions with concentrations higher than 50 mg/mL experienced dissolution when cooled at ambient temperature for less than 30 min.

2.2. Preparation of artificial mucus

The artificial mucus was made by heating HPLC water (HPLC grade, Fisher Scientific, CAS 7732-18-5) on a hot plate at 80 °C while stirring with a magnetic stir bar. An isotonic saline solution was prepared by adding 1.57 g NaCl/$NaHCO_3$ mixture (Minimum of 70 % NaCl, Ayrsaline nasal rinse packet; B.F. Ascher and Co., Inc.; Lenexa, KS) to 177 mL 80 °C HPLC water. To increase the surface tension, sodium dodecyl sulfate surfactant (BioXtra, >99.0 %, Sigma Aldrich, CAS 151-21-3) was added to the saline solution in the amount of 5 mM and mixed thoroughly. Next, 1 wt% locust bean gum (LBG, from *Ceratonia siliqua* seeds, Sigma Aldrich, CAS 9000-40-2) was added dropwise to the saline solution until the LBG was fully dissolved [37]. The artificial mucus gel became more viscous with cooling, ultimately solidifying into a semi-solid gel.

2.3. FTIR spectroscopy

Fourier transform infrared spectroscopy was performed using a Nicolet 6700 spectrometer (Thermo Electron Corporation) and Omnic software (version 8.1.10, Thermo Fisher Scientific). Attenuated total reflectance (ATR-FTIR) spectra were collected with a ZnSe crystal with a liquid nitrogen-cooled MCT-A* (mercury-cadmium-telluride) detector and a Pike Technologies Veemax II accessory, with the angle of incidence set to 60°. Pike Technologies also produced the liquid retainer, used to contain liquid samples on top of the ATR crystal.

2.4. Data collection

Drug diffusion in mucus was monitored and evaluated using FTIR spectroscopy. The artificial mucus layer was placed in a reservoir, and a spectrum was collected to serve as a baseline standard for comparison to time-resolved spectra. Then a layer of drug-doped IPA solution was placed on top of the mucus layer. A schematic of this setup is shown in Fig. 2.

3. Theory and calculations

3.1. FTIR peak height correlation

Spectra were collected at constant time intervals of 60 seconds and monitored for changes in characteristic spectral peaks corresponding to functional groups present in the drugs. As time progressed peaks corresponding to the drug-doped solution appeared, increasing in absorbance as the concentration increased at the crystal's surface. The system reached equilibrium after some time,

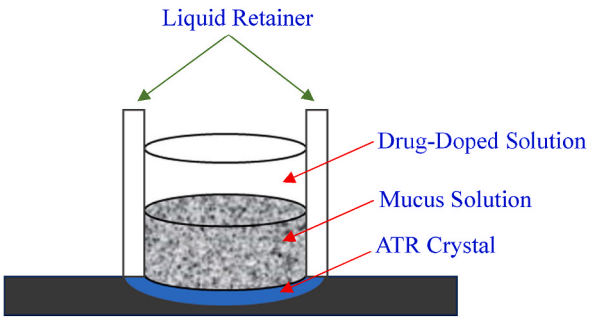

Fig. 2. Schematic of the experimental ATR-FTIR diffusion apparatus.

indicated by a diffusant's characteristic peak height reaching steady state. Fig. 3 displays a time-resolved ATR-FTIR spectra for a 25 mg/mL theophylline/IPA solution diffusing through artificial mucus. The baseline spectrum (t = 0 minutes) is a scan of neat artificial mucus.

3.2. Diffusion model

Fick's second law of diffusion, a one-dimensional continuity equation for unsteady state molecular diffusion without convective diffusion [20,21], was used to analyze the effective diffusivity (neglecting multicomponent effects) of the various drug-IPA solutions through the artificial mucus layer. The equation for Fick's second law of diffusion in terms of concentration can be seen in Equation (1.1) [20,38], where C is the concentration per unit volume of the diffusant, t is time, x is position, and D is the effective diffusion coefficient.

$$\frac{\partial C}{\partial t} = \mathrm{D}\,\frac{\partial^2 C}{\partial x^2} \qquad \text{Eq.1.1}$$

For the case of a planar semi-infinite sheet with fixed thickness and constant concentration maintained at the boundary, Crank derived a solution to Fick's second law of diffusion using the Laplace transform method [25,39]. Fig. 4 depicts a schematic representation of the ATR-FTIR diffusion apparatus and experimental setup. Assuming a planar geometry with fixed mucus layer thickness, h, constant diffusant concentration, C_0, maintained at the drug-mucus interface, and no diffusion is occurring throughout the mucus layer initially or across the mucus-FTIR crystal interface ($x=0$) for any given time, the following two boundary conditions shown in Equations (1.2) and (1.3) can be applied [20]. Crank's trigonometric series solution to Fick's second law of diffusion as it relates to a planar semi-infinite sheet is shown in Equation (1.4) [25,39].

Boundary Condition 1:

$$C = C_0 \; at \; x = \mathrm{h}, t \geq 0 \qquad \text{Eq. 1.2}$$

Boundary Condition 2:

$$\frac{\partial C}{\partial x} = 0 \; at \; x = 0, t \geq 0 \qquad \text{Eq. 1.3}$$

$$C = C_0 - \frac{4C_0}{\pi}\sum_{n=0}^{\infty}\frac{(-1)^n}{2n+1}\exp\left(\frac{-D(2n+1)^2\pi^2 t}{4h^2}\right)\cos\frac{(2n+1)\pi x}{2h} \qquad \text{Eq. 1.4}$$

In the above equation, C_0 is the known loaded drug/diffusant concentration, C is the concentration measured at the mucus-drug solution interface, and x is the depth of penetration of the IR source beam into the mucus layer. Normalizing the experimentally-determined concentration at the mucus-drug solution interface by the known initial drug/diffusant concentration, a modified form

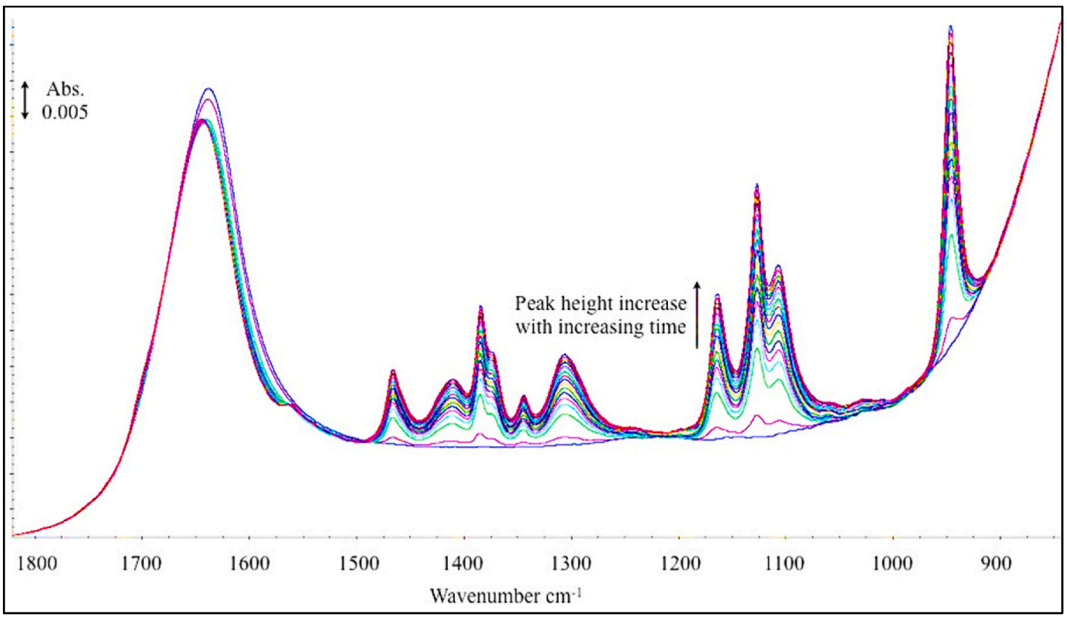

Fig. 3. Time-resolved ATR-FTIR spectra collected over 600 seconds for the diffusion of a 25 mg/mL theophylline/IPA solution through a 3.5 mm artificial mucus layer.

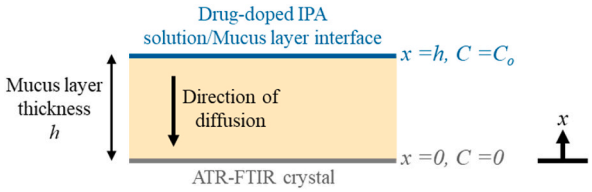

Fig. 4. Schematic representation of boundary conditions applied to the unsteady state Fickian mucus-drug diffusion system. The drugs molecularly diffuse through the mucus layer from the drug-doped IPA solution/mucus interface to the ATR-FTIR crystal/mucus layer interface in the x-direction.

of Eq. (1.4) can be obtained and is shown in Eq. (1.5).

$$\frac{C}{C_o} = 1 - \frac{4}{\pi}\sum_{n=0}^{\infty}\frac{(-1)^n}{2n+1}\exp\left(\frac{-D(2n+1)^2\pi^2 t}{4h^2}\right)\cos\frac{(2n+1)\pi x}{2h} \qquad \text{Eq. 1.5}$$

Through nonlinear regression analysis, the diffusivity coefficient, D, can be approximated. For this work, the mucus layer thickness is h = 0.15 cm, the depth of penetration of the IR source into the mucus layer is $x = 8.78 \times 10^{-5}$ cm based on the selected IR peak absorbance (1645 cm^{-1}), and the refractive indices of the ATR crystal and the mucus layer are 2.40 and 1.76, respectively [20,25]. In addition, the summation in Eq. (1.5) was truncated at $n = 500$. Selecting some initial fixed value of D allows for comparing the experimental and model values for $\frac{C}{C_o}$ at a specific time t. The minimization of the squared error, SE, was then used as a metric to finalize the value of D and determine the consistency of the model in comparison to experimental measurements and is given by the equation [40]:

$$SE = \sum_{k=1}^{K}\left(E_{t(k)} - M_{t(k)}\right)^2 \qquad \text{Eq. 1.6}$$

Here, $E_{t(k)}$ is the experimentally-determined $\frac{C}{C_o}$ value at some time $t(k)$. For example, for measurements determined at times t = 0, 30, 60, 90, and 200 seconds where $t(1) = 0$, $t(2) = 30$, $t(3) = 60$, $t(4) = 90$ and $t(5) = 200$, then $E_{t(1)}$, $E_{t(2)}$ $E_{t(3)}$ $E_{t(4)}$ $E_{t(5)}$ would be the experimental values of $\frac{C}{C_o}$ at 0, 30, 60, 90, and 200 seconds. Similarly, $M_{t(k)}$ would be the model values of $\frac{C}{C_o}$ given Eq. (1.5) evaluated at similar fixed times, $t(k)$. Explicitly, SE Eq. (1.6) can be expressed as

$$SE(D) = \sum_{k=1}^{K}\left(E_{t(k)} - 1 + \frac{4}{\pi}\sum_{n=0}^{\infty}\frac{(-1)^n}{2n+1}\exp\left(\frac{-D(2n+1)^2\pi^2 t(k)}{4h^2}\right)\cos\frac{(2n+1)\pi x}{2h}\right)^2 \qquad \text{Eq. 1.7}$$

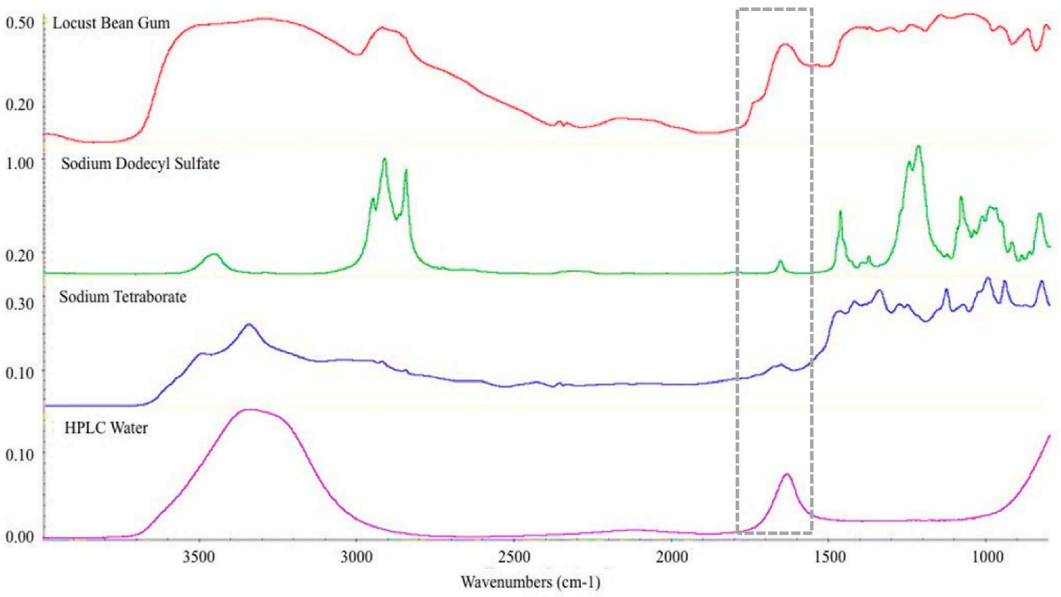

Fig. 5. Stacked FTIR spectra of the artificial mucus components. Boxed peaks around ~1640 cm^{-1} are of interest due to the overshadowing the peaks have on secondary amine peaks in the drugs.

where Eq. (1.5) for the model $\frac{C}{C_o}$ was inserted into the $M_{t(k)}$ term of Eq. (1.6). In this equation, the only parameter that will change the value of the *SE* is the diffusivity coefficient *D*, and therefore Eq (1.7) can be considered as a function of the diffusivity constant, *SE*(*D*). As minimizing the squared error is desired, it can be asserted that the true value of *D* will minimize the value of the squared error. The value of *D* that minimizes the SE was determined using non-linear regression software. Using this method, diffusion coefficients for albuterol and theophylline were determined. Figs. 7 and 8 show the ATR-FTIR peak height-concentration calibration curve and diffusion coefficients determination through the minimization of the standard error function, respectively.

4. Results and discussion

Examination of Fig. 3 reveals the IR absorbance peaks that appear and subsequently increase in height with time as the drug-IPA solution diffuses through the mucus layer. These peaks represent the IR signatures for the solvent (IPA) and the drug (theophylline), with a majority of these peaks corresponding to IPA. While theophylline is present in the solution, the concentration and relatively low absorption make it difficult to differentiate from the IPA peaks. In addition, the peak at ~1645 cm^{-1} corresponding to the secondary amines in theophylline [41], is overshadowed by the large peak at ~1640 cm^{-1} corresponding to ring stretching of galactose and mannose [42] in the LBG-based mucus. Stacked ATR-FTIR spectra of the individual mucus components can be seen in Fig. 5. Fig. 6 shows a comparison of neat IPA (baseline spectrum) with drug-doped IPA solutions, highlighting spectral peaks specific to theophylline. Within the 1750-1500 cm^{-1} range, several peaks are present and attributed to the theophylline-doped IPA solutions, which were not present in neat IPA.

Albuterol-doped IPA solutions also contained the ~1645 cm^{-1} peak. Peaks in this wavenumber range correspond to secondary amines [43,44] that are present in both chemical structures. Theophylline contains primary, secondary, and tertiary amines and albuterol contains secondary amines (see Fig. 1). The peak height tool was then used to calculate the peak height of the drug peaks at ~1645 cm^{-1}. Peak heights were then converted to drug concentrations using a calibration curve before using the experimental concentration to determine an average diffusivity coefficient.

The ATR-FTIR peak height-concentration calibration curves for the drug-doped IPA solutions were prepared by first determining the height of the 1645 cm^{-1} peak for each drug solution ranging in concentration from 0 to 75 mg/mL. The measured peak heights for the drug were then plotted as a function of drug solution concentration, and the data set was fitted to a linear function, as predicted by Beer's Law [19]. The fitted concentration profiles for theophylline and albuterol in IPA are shown in Fig. 7a and b, respectively.

Next, the IR absorbance peak heights of the drugs were measured for each of the time-resolved spectra for drug diffusion through the mucus layer. To evaluate the time-resolved spectra for increasing concentrations of drug-doped solutions, the ATR-FTIR spectrum for the neat mucus solution was subtracted from the time-resolved spectra. Using the subtraction processing method available within the Omnic software, one spectrum can be subtracted from another to identify differences more clearly. In this case, the drug-doped IPA solution concentration could be clearly determined by the subtraction spectra. For example, a spectrum for theophylline-IPA solution through mucus at a time of 4000 s would look like a neat mucus solution with several IPA peaks appearing. Since it is known that theophylline is in the IPA solution and that a strong peak of mucus overshadows the traceable peak for theophylline that is present, it is necessary to remove any peaks corresponding to mucus in order to observe the theophylline peak. The subtraction tool uses the neat mucus spectrum to identify the peaks corresponding to mucus and remove them from the time-resolved spectrum, resulting in a spectrum that corresponds to the theophylline-IPA solution that has presently diffused through the mucus to the surface of the ATR crystal. The peak height of the theophylline peak can then be evaluated and subsequently used for further calculations. This evaluation

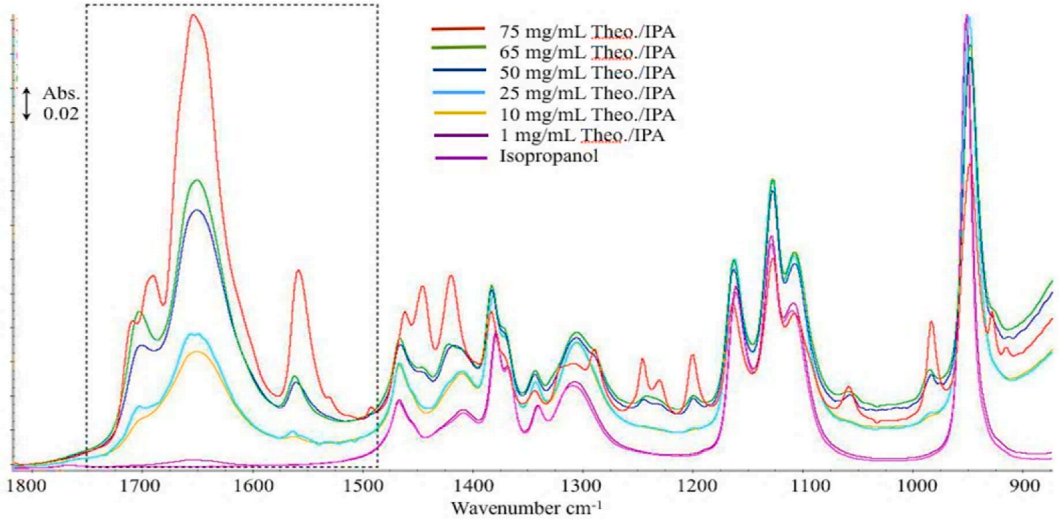

Fig. 6. ATR-FTIR spectra for a concentration series of theophylline in IPA.

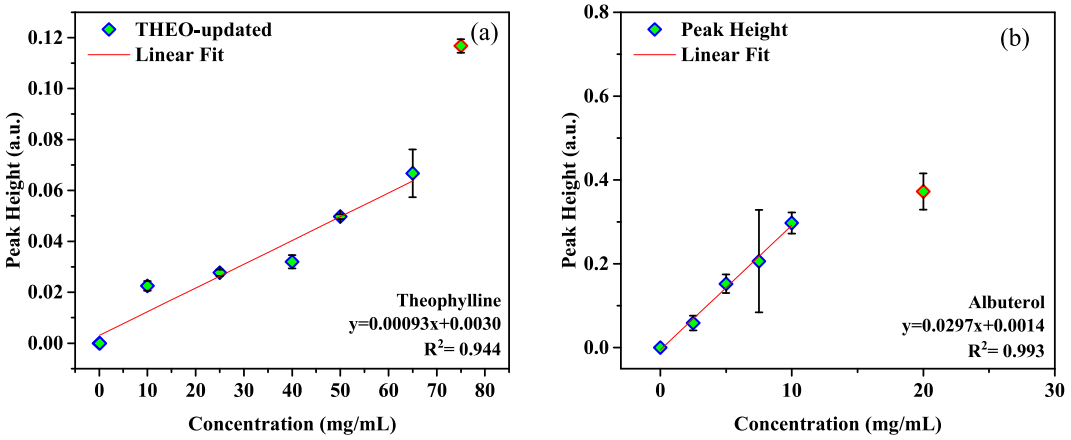

Fig. 7. Drug concentration profiles for (a) theophylline and (b) albuterol based on measured ATR-FTIR peak heights were fit to a linear function (y = 0.00093x-0.0030 (R^2 = 0.944) and y = 0.0297x+0.0014 (R^2 = 0.993) for theophylline and albuterol, respectively). Standard deviations for the peak height measurements ranged from ±0.001 to ±0.009 a.u. for theophylline and ±0.018 to ±0.122 a.u. for albuterol. The high concentration data points for both theophylline and albuterol were found to be outliers, outside the linear absorbance region, and omitted from the line fitting.

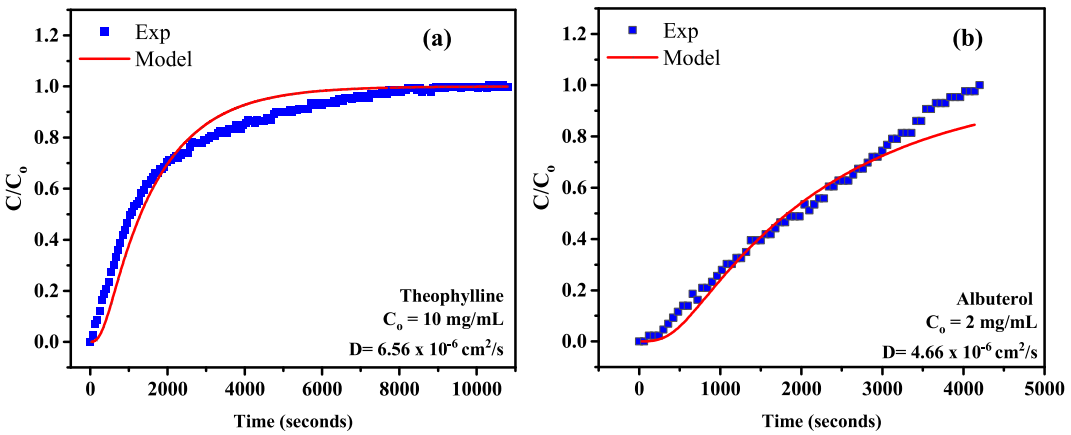

Fig. 8. Comparison of experimental (blue squares) and calculated concentrations (red line) for (a) 10 mg/mL theophylline-IPA solution and (b) 2 mg/mK albuterol-IPA solution diffusing through an artificial mucus layer. (For interpretation of the references to colour in this figure legend, the reader is referred to the Web version of this article.)

method was used to find the peak height of the drug at each time interval of diffusion through the mucus layer. The peak height data as a function of time was then converted to drug concentration using the fitted peak height-concentration relationship determined previously (Fig. 7) and solving for the "x" concentration variable.

The overall square error (Eq (1.6)) could then be minimized using the determined drug concentration profiles through mucus with time compared to the model diffusion (Eq (1.5)). Fig. 8 illustrates the accuracy of Crank's solution for unsteady state Fickian diffusion as compared to the experimental data for drug diffusion through the mucus layer using the calculated diffusivity constant which minimized the SE (Eq (1.6)). As it is important to validate the numerical model in comparison to the experimental data for different conditions [45], the experimental and model concentration profiles are provided for theophylline-IPA (Fig. 8a) and albuterol-IPA (Fig. 8b) solutions through mucus. Overall, the experimental data for theophylline follows the shape of the modeled curve well, and the small deviations observed between the model and experimental profiles are consistent with other systems observed in the literature [23,25]. The deviations may also be a result of the slight non-linearity between lower concentrations and absorbance cited

Table 1
Measured diffusivity coefficients for theophylline and albuterol in artificial mucus.

Drug	Solution Concentration (mg/mL)	Total Data Collection Time (s)	Mucus Layer Thickness (cm)	Diffusivity (10^{-6} cm^2/s)	Standard Deviation
Theophylline	5–25	6,900–10,800	0.15–0.35	5.5–8.0	± 0.72
Albuterol	2–30	1,500–5,100	0.15–0.40	1.6–4.9	± 5.4

for Beer's Law [46–48]. The nonlinear regression results for albuterol also show good agreement between the experimental and model profiles, although it is noted that this experiment was not carried out to equilibrium.

Evaluation of diffusivity coefficients to minimize the SE between the experimental data and Crank's model determined the diffusivity of theophylline (in IPA) through the mucus, with diffusivity coefficients ranging from 5.5 to 8.0 $\times$ 10^{-6} cm^2/s. Albuterol resulted in a broader range of diffusion and produced diffusion coefficients ranging from 1.6 to 4.9 $\times$ 10^{-6} cm^2/s. Table 1 summarizes the range of diffusion coefficients measured using the ATR-FTIR diffusion method for theophylline and albuterol.

The diffusion coefficient values for aerosol drugs through mucus range from 4.9 to 9.6 $\times$ 10^{-6} cm^2/s, and specific examples are given below. In the literature, homologous radiolabeled carbohydrates glucuronic acid, glucosamine, and mannitol diffused through native porcine mucus produced diffusivity values ranging from 7 to 9 $\times$ 10^{-6} cm^2/s, while the lipophilic molecule testosterone produced a diffusivity of 3 $\times$ 10^{-6} cm^2/s [16,49]. Drugs such as isonicotinic acid hydrazide, sodium p-aminosalicylate, pentamidine, pyrazinamide, and rifampicin produced diffusivity values ranging from 5.07 to 7.62 $\times$ 10^{-6} cm^2/s when diffused through reconstituted mucus in Side-by-Side® diffusion cell [50]. Theophylline diffusion coefficients have been reported as 2 $\times$ 10^{-6} cm^2/s [51] and 1.83 $\times$ 10^{-5} - 5.83 $\times$ 10^{-9} cm^2/s [52], which are in reasonable agreement with the diffusion coefficients determined in this study. Similarly, albuterol diffusion coefficients ranging from 9.1 x 10^{-7} and 6.2 x 10^{-6} cm^2/s have been reported [53,54] and agree with the results from this study. Even though equilibrium was not reached during the albuterol experiments, the results still indicate accurate diffusivity values obtained for experiments lasting <1 h (before reaching equilibrium) and even for experiments at low diffusant concentrations. Based on literature findings, the range of experimental diffusivity values measured in this work appears to be appropriate for the materials tested thereby validating the FTIR-based data collection and analysis methods. This work provides an FTIR spectroscopic technique paired with Fickian one-dimensional transient transport modeling as a widely available instrumental and computational methodology to estimate the effective diffusion coefficient of inhalation drugs through a mucosal solution.

5. Conclusions

In our work, we report a synthetic route to prepare an artificial mucus capable of modeling the diffusion behavior of asthma medication. Specifically, we have adapted an analytical modeling approach to study the diffusion coefficients of theophylline and albuterol. Also, time-resolved Fourier transform infrared (FTIR) spectroscopy was employed to monitor the diffusion process as an important tool in the evaluation and development of both administered drugs on the artificial mucus layer. Our results reveal that the calculated average diffusivity coefficients of theophylline and albuterol through artificial mucus are accurate representations of the changes observed in human pulmonary mucus due to the drags used for asthma treatment. FTIR data exhibited expected elevations in peak heights of the drug-specific peak, adhering to the expected trend of a continuous rise in peak height over time, followed by an equilibrium phase. While the diffusivities were expected to be slightly lower, the data exhibited consistency in the diffusivity coefficient values, independent of variations in mucus layer thickness, or the duration of data collection. The diffusivity coefficients for theophylline (6.56 $\times$ 10^{-6} cm^2/s, 10 mg/mL initial concentration) and albuterol (4.66 $\times$ 10^{-6} cm^2/s, 2 mg/mL initial concentration) obtained for artificial mucus, closely aligned with literature reports validates the analytical and experimental approach. This study holds significant potential in developing convenient models to understand drug diffusion in mucus for asthma treatment and drug development.

Data availability

Data will be made available on request.

CRediT authorship contribution statement

Ashley C. Wynne: Writing – original draft, Methodology, Investigation, Formal analysis. **Brandon S. Abbott:** Writing – review & editing, Formal analysis. **Reza Niazi:** Formal analysis. **Kayla Foley:** Writing – review & editing, Formal analysis. **Keisha B. Walters:** Writing – review & editing, Supervision, Project administration, Methodology, Funding acquisition, Conceptualization.

Declaration of competing interest

The authors declare that they have no known competing financial interests or personal relationships that could have appeared to influence the work reported in this paper.

Acknowledgements

We would like to acknowledge the National Science Foundation for supporting this project [EPS-0903787]. The Southeastern Conference (SEC) Emerging Scholars program is thanked for providing partial funding for Kayla Foley on this project. We appreciate the efforts of undergraduate researcher Kiefer Slaton for his assistance in collecting a portion of the FTIR data.

Nomenclature

ATR-FTIR	attenuated total reflectance Fourier transform infrared spectroscopy
IPA	isopropyl alcohol
D [cm^2/s]	diffusion coefficient
t [s]	time
x [cm]	depth in mucus layer
C [mg/cm^3]	drug concentration in the mucus layer at t and x
h [cm]	height of mucus layer
Co [mg/cm^3]	initial drug solution concentration maintained at the drug solution-mucus interface at h
dp [cm]	depth of penetration of the infrared beam into the mucus layer
n [unitless]	integer
SE [unitless]	squared error as described in Eq. 1.6
$E_{t(k)}$ [unitless]	experimental concentration profile $\frac{C}{C_o}$ at time *t(k)*
$M_{t(k)}$ [unitless]	model concentration profile $\frac{C}{C_o}$ at time *t(k)*
k [unitless]	integer

References

[1] B.J. Dierick, et al., Burden and socioeconomics of asthma, allergic rhinitis, atopic dermatitis and food allergy, Expert Rev. Pharmacoecon. Outcomes Res. 20 (2020) 437–453.
[2] T. Nurmagambetov, R. Kuwahara, P. Garbe, The economic burden of asthma in the United States, 2008–2013, Annals of the American Thoracic Society 15 (2018) 348–356.
[3] Collaborators, G. C. R. D, Global, regional, and national deaths, prevalence, disability-adjusted life years, and years lived with disability for chronic obstructive pulmonary disease and asthma, 1990–2015: a systematic analysis for the Global Burden of Disease Study 2015, Lancet Respir. Med. 5 (2017) 691.
[4] T. Volsko, M. Reed, Drugs used in the treatment of asthma: a review of clinical pharmacology and aerosol drug delivery, Respir. Care Clin. 6 (2000) 41–55.
[5] M. Ballmann, A. Smyth, D.E. Geller, Therapeutic approaches to chronic cystic fibrosis respiratory infections with available, emerging aerosolized antibiotics, Respir. Med. 105 (2011) S2–S8.
[6] H.-K. Chan, Dry powder aerosol delivery systems: current and future research directions, J. Aerosol Med. 19 (2006) 21–27.
[7] R. Dhand, Inhaled drug therapy 2016: the year in review, Respir. Care 62 (2017) 978–996.
[8] A.J. Hickey, Delivery of drugs by the pulmonary route, Drugs Pharmaceut. Sci. 121 (2002) 479–500.
[9] A.J. Hickey, H.M. Mansour, in: Modern Pharmaceutics vol. 2, CRC Press, 2016, pp. 209–238.
[10] J.S. Patton, Mechanisms of macromolecule absorption by the lungs, Adv. Drug Deliv. Rev. 19 (1996) 3–36.
[11] T. Velkov, N.A. Rahim, Q.T. Zhou, H.-K. Chan, J. Li, Inhaled anti-infective chemotherapy for respiratory tract infections: successes, challenges and the road ahead, Adv. Drug Deliv. Rev. 85 (2015) 65–82.
[12] K. Khanvilkar, M.D. Donovan, D.R. Flanagan, Drug transfer through mucus, Adv. Drug Deliv. Rev. 48 (2001) 173–193.
[13] N. El-Gendy, W. Pornputtapitak, C. Berkland, Nanoparticle agglomerates of fluticasone propionate in combination with albuterol sulfate as dry powder aerosols, Eur. J. Pharmaceut. Sci. 44 (2011) 522–533.
[14] J. Todoroff, R. Vanbever, Fate of nanomedicines in the lungs, Curr. Opin. Colloid Interface Sci. 16 (2011) 246–254.
[15] S.K. Lai, Y.-Y. Wang, J. Hanes, Mucus-penetrating nanoparticles for drug and gene delivery to mucosal tissues, Adv. Drug Deliv. Rev. 61 (2009) 158–171.
[16] A.W. Larhed, P. Artursson, J. Gråsjö, E. Björk, Diffusion of drugs in native and purified gastrointestinal mucus, J. Pharmaceut. Sci. 86 (1997) 660–665.
[17] D.A. Norris, P.J. Sinko, Effect of size, surface charge, and hydrophobicity on the translocation of polystyrene microspheres through gastrointestinal mucin, J. Appl. Polym. Sci. 63 (1997) 1481–1492.
[18] L.R. Shaw, W.J. Irwin, T.J. Grattan, B.R. Conway, The influence of excipients on the diffusion of ibuprofen and paracetamol in gastric mucus, Int. J. Pharm. 290 (2005) 145–154.
[19] T. Hallinan Jr D, De Angelis, M. G, M. Giacinti Baschetti, C. Sarti G, Y.A. Elabd, Non-fickian diffusion of water in nafion, Macromolecules 43 (2010) 4667–4678.
[20] D.T. Hallinan, Y.A. Elabd, Diffusion and sorption of methanol and water in nafion using time-resolved fourier transform infrared− attenuated total reflectance spectroscopy, J. Phys. Chem. B 111 (2007) 13221–13230.
[21] Y.A. Elabd, M.G. Baschetti, T.A. Barbari, Time-resolved Fourier transform infrared/attenuated total reflection spectroscopy for the measurement of molecular diffusion in polymers, J. Polym. Sci. B Polym. Phys. 41 (2003) 2794–2807.
[22] W. McAuley, et al., ATR-FTIR spectroscopy and spectroscopic imaging of solvent and permeant diffusion across model membranes, Eur. J. Pharm. Biopharm. 74 (2010) 413–419.
[23] K. Kim, D.T. Hallinan Jr., Lithium salt diffusion in diblock copolymer electrolyte using fourier transform infrared spectroscopy, J. Phys. Chem. B 124 (2020) 2040–2047, https://doi.org/10.1021/acs.jpcb.9b11446.
[24] Y. Dong, L. Hou, P. Wu, Exploring the diffusion behavior of urea aqueous solution in the viscose film by ATR-FTIR spectroscopy, Cellulose 27 (2020) 2403–2415, https://doi.org/10.1007/s10570-020-02997-y.
[25] A. Watkinson, J. Hadgraft, K. Walters, K. Brain, Measurement of diffusional parameters in membranes using ATR-FTIR spectroscopy, Int. J. Cosmet. Sci. 16 (1994) 199–210.
[26] Y. Wang, J. Qian, M. Fang, R. Guo, Y. Shi, The effects of monomer on the diffusion behavior of drug molecules in acrylic pressure-sensitive adhesive, Mater. Res. Express 8 (2021), https://doi.org/10.1088/2053-1591/abef3e, 035307.
[27] M. Karimi, A.A. Tashvigh, F. Asadi, F.Z. Ashtiani, Determination of concentration-dependent diffusion coefficient of seven solvents in polystyrene systems using FTIR-ATR technique: experimental and mathematical studies, RSC Adv. 6 (2016) 9013–9022.
[28] B.M. Carter, B.M. Dobyns, B.S. Beckingham, D.J. Miller, Multicomponent transport of alcohols in an anion exchange membrane measured by in-situ ATR FTIR spectroscopy, Polymer 123 (2017) 144–152.
[29] M. Soniat, F.A. Houle, Swelling and diffusion during methanol sorption into hydrated nafion, J. Phys. Chem. B 122 (2018) 8255–8268.
[30] Y. Cu, W.M. Saltzman, Mathematical modeling of molecular diffusion through mucus, Adv. Drug Deliv. Rev. 61 (2009) 101–114, https://doi.org/10.1016/j.addr.2008.09.006.
[31] J.M. Newby, et al., Technological strategies to estimate and control diffusive passage times through the mucus barrier in mucosal drug delivery, Adv. Drug Deliv. Rev. 124 (2018) 64–81, https://doi.org/10.1016/j.addr.2017.12.002.
[32] L. Kaler, et al., Influenza A virus diffusion through mucus gel networks, Commun. Biol. 5 (2022) 249, https://doi.org/10.1038/s42003-022-03204-3.

[33] S.K. Lai, et al., Rapid transport of large polymeric nanoparticles in fresh undiluted human mucus, Proc. Natl. Acad. Sci. USA 104 (2007) 1482–1487, https://doi.org/10.1073/pnas.0608611104.
[34] D.H. Owen, E.N. Dunmire, A.M. Plenys, D.F. Katz, Factors influencing nonoxynol-9 permeation and bioactivity in cervical mucus, J. Contr. Release 60 (1999) 23–34.
[35] P. Occhipinti, P.C. Griffiths, Quantifying diffusion in mucosal systems by pulsed-gradient spin-echo NMR, Adv. Drug Deliv. Rev. 60 (2008) 1570–1582, https://doi.org/10.1016/j.addr.2008.08.006.
[36] A.L. Cornell, Studies in Applied Materials Science: Drug-Biofluid Interactions and Light-Emitting Polymer Films, Mississippi State University, 2012.
[37] M.A. Hasan, C.F. Lange, M.L. King, Effect of artificial mucus properties on the characteristics of airborne bioaerosol droplets generated during simulated coughing, J. Non-Newtonian Fluid Mech. 165 (2010) 1431–1441.
[38] R. Bird, E. Lightfoot, W. Stewart. Transport Phenomena, Wiley & Sons, 1960.
[39] J. Crank. The mathematics of diffusion, Oxford University Press, 1979.
[40] H.H. Huang, C.K. Hsiao, S.Y. Huang, in: Penelope Peterson, Eva Baker, Barry McGaw (Eds.), International Encyclopedia of Education, 3rd ed., Elsevier,, 2010, pp. 339–346.
[41] E. Pretsch, P. Bühlmann, Affolter. C.,Structure Determination of Organic Compounds, Springer, 2000.
[42] J. Wang, P. Somasundaran, Study of galactomannose interaction with solids using AFM, IR and allied techniques, J. Colloid Interface Sci. 309 (2007) 373–383.
[43] T.J. Bruno, P.D. Svoronos, CRC Handbook of Fundamental Spectroscopic Correlation Charts, CRC Press, 2005.
[44] R.M. Silverstein, G.C. Bassler, Spectrometric identification of organic compounds, J. Chem. Educ. 39 (1962) 546.
[45] W.-B. Ye, M. Arıcı, Redefined interface error, 2D verification and validation for pure solid-gallium phase change modeling by enthalpy-porosity methodology, Int. Commun. Heat Mass Tran. 147 (2023) 106952, https://doi.org/10.1016/j.icheatmasstransfer.2023.106952.
[46] A.Y. Tolbin, V.E. Pushkarev, L.G. Tomilova, N.S. Zefirov, Threshold concentration in the nonlinear absorbance law, Phys. Chem. Chem. Phys. 19 (2017) 12953–12958.
[47] T.G. Mayerhöfer, A. Dabrowska, A. Schwaighofer, B. Lendl, J. Popp, Beyond beer's law: why the index of refraction depends (almost) linearly on concentration, ChemPhysChem 21 (2020) 707–711.
[48] T.G. Mayerhöfer, J. Popp, Beyond beer's law: revisiting the lorentz-lorenz equation, ChemPhysChem 21 (2020) 1218–1223.
[49] A.W. Larhed, P. Artursson, E. Björk, The influence of intestinal mucus components on the diffusion of drugs, Pharmaceut. Res. 15 (1998) 66–71.
[50] P.G. Bhat, D.R. Flanagan, M.D. Donovan, The limiting role of mucus in drug absorption: drug permeation through mucus solution, Int. J. Pharm. 126 (1995) 179–187.
[51] M. Grassi, D. Voinovich, E. Franceschinis, B. Perissutti, J. Filipovic-Grcic, Theoretical and experimental study on theophylline release from stearic acid cylindrical delivery systems, J. Contr. Release 92 (2003) 275–289.
[52] C. Alvarez-Lorenzo, J. Gomez-Amoza, R. Martınez-Pacheco, C. Souto, A. Concheiro, Microviscosity of hydroxypropylcellulose gels as a basis for prediction of drug diffusion rates, Int. J. Pharm. 180 (1999) 91–103.
[53] Y.B. Bannon, J. Corish, O.I. Corrigan, J.G. Masterson, Iontophoretically induced transdermal delivery of salbutamol, Drug Dev. Ind. Pharm. 14 (1988) 2151–2166, https://doi.org/10.3109/03639048809152008.
[54] G. Imanidis, R. Imboden, Utilizing vehicle imbibition by a microporous membrane and vehicle viscosity to control the release rate of salbutamol, Eur. J. Pharm. Biopharm. 47 (1999) 283–287, https://doi.org/10.1016/S0939-6411(99)00004-1.